doi: 10.4149/gpb_2026011

USP7/SETDB1 promotes non-small cell lung cancer progression by regulating ferroptosis *via* NRF2/SLC7A11/GPX4 axis

Hongpei Zhang[1], Yanfeng Fang[1], Xinxin Wang[1], Wenting Wu[1], Dandan Li[1] and Yuan Zhang[1]

[1] *Department of Respiratory and Critical Care Medicine, Tangdu Hospital of Air Force Military Medical University, Baqiao District, Xi'an, China*

Abstract. Non-small cell lung cancer (NSCLC) is a malignant tumor with high morbidity and mortality. Given the reported associations of both SET domain bifurcated histone lysine methyltransferase 1 (SETDB1) with various cancers and ubiquitin-specific protease 7 (USP7) with NSCLC progression, this study aims to elucidate the role of SETDB1 and USP7 in NSCLC progression. mRNA and protein levels were measured by qRT-PCR and Western blot, respectively. Cell biological phenotypes were evaluated using MTT, EdU, flow cytometry, transwell, and sphere formation assays. Ferroptosis was analyzed by measuring Fe^{2+}, MDA GSH, and ROS levels. Relationship between USP7 and SETDB1 was examined through Co-IP, cycloheximide (CHX) chase, and deubiquitination assays. Xenograft tumor models were established to investigate the role of SETDB1 and USP7 in NSCLC *in vivo*. In NSCLC tissues and cells, SETDB1 levels were elevated. Knockdown of SETDB1 inhibited NSCLC cell viability, proliferation, invasion, and sphere formation ability, while promoting apoptosis and ferroptosis. Mechanistically, USP7 enhanced the stability of SETDB1 protein by its deubiquitination. USP7 knockdown suppressed NSCLC cell biological behavior by downregulating SETDB1. Moreover, USP7 knockdown repressed *in vivo* tumor growth of NSCLC. Taken together, USP7 suppresses ferroptosis and enhances growth in NSCLC cells by stabilizing SETDB1 protein through deubiquitination.

Key words: NSCLC — USP7 — SETDB1 — Ferroptosis — Biological behavior — Ubiquitination

Introduction

Lung cancer is a commonly diagnosed malignancy worldwide, and GLOBOCAN database shows that there were 2.2 million new cases of lung cancer globally by 2020 (Ferlay et al. 2021). Lung cancer is mainly divided into small cell lung cancer and non-small cell lung cancer (NSCLC), among which NSCLC accounts for about 85% (Wang et al. 2025). Although diagnostic and therapeutic strategies for NSCLC have advanced in recent years, the 5-year survival rate remains unsatisfactory (Kandemir and Demir 2024). Therefore, there is an urgent need to elucidate the molecular pathophysiology of NSCLC for identifying novel therapeutic targets.

SET domain bifurcated histone lysine methyltransferase 1 (SETDB1) is chromatin regulator that plays a crucial role in both euchromatic and heterochromatic regions (Hassanie and Penteado 2024). SETDB1 has been observed to be upregulated across multiple cancer types, where it frequently correlates with disease progression (Strepkos and Markouli 2021). For example, SETDB1 overexpression was closely associated with advanced clinical stage and shorter survival in hepatocellular carcinoma, suggesting its potential value as a prognostic biomarker (Wang et al. 2022). Similarly, expression of SETDB1 was increased in metastatic head and neck carcinoma and is associated with shortened survival

Electronic supplementary material. The online version of this article (doi:10.4149/gpb_2026011) contains Supplementary material.

Correspondence to: Yanfeng Fang, Department of Respiratory and Critical Care Medicine, Tangdu Hospital of Air Force Military Medical University, No. 569 Xinsi Road, Baqiao District, Xi'an 710038, China
E-mail: 18066750950@163.com

time (Özdaş 2019). SETDB1 silencing prevented ovarian cancer cell migration and motility by modulating SF3B4 expression and altering the tumor immune microenvironment (Yang H et al. 2024). Deletion of SETDB1 suppressed breast cancer cell proliferation, invasion, and migration *in vitro* and reduced lung metastasis *in vivo*. Mechanistically, SETDB1 exerted these effects by directly binding to the Snail promoter (Yang et al. 2019). Notably, research demonstrated that expression of SETDB1 was related to shorter disease-free survival in stage I NSCLC patients (Lafuente-Sanchis et al. 2016). Moreover, SETDB1 has been found as an oncogene in lung cancer (Rodriguez-Paredes et al. 2014). Despite these observations, the functional roles and molecular mechanisms of SETDB1 in NSCLC progression remain largely uncharacterized.

Ubiquitin-specific protease 7 (USP7), also known as herpesvirus-associated ubiquitin-specific protease (HAUSP), is a well-characterized cysteine protease belonging to the largest subfamily of deubiquitinating enzymes (DUBs) that removes ubiquitin chains from its target proteins to regulate their stability (Carreira and Oliveira 2023). By counteracting ubiquitin-mediated proteasomal degradation, USP7 stabilizes a wide array of substrates, including key regulators such as the tumor suppressor p53 and its negative regulator MDM2, thereby exerting context-dependent effects on cellular processes (Saha and Ghosh 2025). USP7 is critically involved in various biological processes, including epigenetic regulation, DNA repair, cell cycle, and tumorigenesis (Al-Eidan et al. 2022). Notably, USP7 is overexpressed in many types of cancer and is an important regulator in oncogenesis (Saha et al. 2023). For instance, USP7 expression was elevated in NSCLC, and USP7 facilitated proliferation of NSCLC cells by promoting KRAS stability through deubiquitination (Huang et al. 2024). However, the potential interplay between USP7 and SETDB1 in NSCLC remains unexplored.

Table 1. Relationship between SETDB1 expression and clinicopathologic features of non-small-cell lung cancer patients

Characteristics $n = 37$		SETDB1 expression		p value
		low ($n = 18$)	high ($n = 19$)	
Age (years)				0.7431
≤50	16	7	9	
>50	21	11	10	
TNM grade				0.0217*
I+II	17	12	5	
III	20	6	14	
Lymph node metastasis				0.0029*
Positive	20	5	15	
Negative	17	13	4	

TNM, tumor-node-metastasis; * $p < 0.05$.

Building on these findings, this study aims to investigate the functional interplay of USP7 and SETDB1 in NSCLC progression, thereby providing a new theoretical basis and identifying potential therapeutic targets for this disease.

Materials and Methods

Bioinformatics analysis

The SETDB1 expression in lung adenocarcinoma (LUAD) and normal lung tissues was examined using UALCAN-TCGA (https://ualcan.path.uab.edu/analysis.html), UALCAN-CPTAC (https://ualcan.path.uab.edu/analysis-prot.html), and ENCORI (https://starbase.sysu.edu.cn/) databases. Additionally, the TNMplot database (https://tnmplot.com/analysis/) was employed to analyze the SETDB1 levels in NSCLC and normal lung tissues. The potential interaction between USP7 and SETDB1 was predicted using the UbiBrowser database (http://ubibrowser.ncpsb.org.cn/). The correlation between USP7 and SETDB1 expression levels was predicted using ENCORI (https://starbase.sysu.edu.cn/) and GEPIA databases (http://gepia.cancer-pku.cn/), respectively.

Tissue samples

NSCLC tissues and adjacent normal tissues were harvested when patients with NSCLC ($n = 37$) underwent surgical treatment at Tangdu Hospital of Air Force Military Medical University. All the patients had not received chemotherapy or radiotherapy before the surgery. All tumor and non-tumor tissues were independently confirmed by two pathologists. The clinicopathological parameters of the patients were summarized in Table 1. The samples were stored at −80°C. Signed informed consents were offered by all participants. The present study was approved by the Ethics Committee of Tangdu Hospital of Air Force Military Medical University.

Detection of mRNA expression

The tissue and cell samples were lysed using TRIZOL solution (Kanglang Biotechnology Co., Ltd., Shanghai, China) to extract total RNA based on the manufacturer's guidelines. Subsequently, the RNA concentration and purity were examined by NanoDrop2000c (Thermo Fisher Scientific, Waltham, MA, USA). The extracted RNA was then reverse transcribed into cDNA using the SuperScript VILO cDNA Synthesis Kit (Thermo Fisher Scientific, Waltham, MA, USA). Quantitative real-time polymerase chain reaction (qRT-PCR) was carried out with TB Green PrimeScript RT-PCR Kit II (Takara, Beijing, China). GAPDH was used as an

internal control and the fold change of mRNA expression was calculated using the $2^{-\Delta\Delta Ct}$ method. The forward and reverse primers used were as follows: SETDB1, 5'-TTGGATTTGACCCCGTCAGG-3' and 5'-CAACGTGAGCCACCTCAGAT-3'; GAPDH, 5'-AATGGGCAGCCGTTAGGAAA-3' and 5'-GCGCCCAATACGACCAAATC-3'; and USP7, 5'-AATGGGAATGTGGCCCTGAG-3' and 5'-GGGTAAACCGCACTGTGAGA-3'.

Detection of protein levels

The protein was extracted with RIPA solution (Invitrogen, Carlsbad, CA, USA) based on the instruction of manufacturer. The BCA assay kit (Vazyme, Nanjing, China) was employed to analyze the protein concentration. Following that, proteins (30 μg per lane) were separated by 10% sodium dodecyl sulfate-polyacrylamide gel electrophoresis (SDS-PAGE) and then transferred onto nitrocellulose membranes (Beyotime, Shanghai, China). After blocking with 5% non-fat milk, the proteins were incubated with anti-SETDB1 (ab300573, 1:1000, Abcam, Cambridge, MA, USA), anti-GAPDH (ab313651, 1:3000, Abcam), anti-USP7 (ab264422, 1:1000, Abcam), anti-nuclear factor erythroid 2-related factor 2 (NRF2) (ab137550, 1:3000, Abcam), anti-glutathione peroxidase 4 (GPX4) (ab41787, 1:2000, Abcam), and anti-solute carrier family 7 member 11 (SLC7A11) (ab300667, 1:1000, Abcam) at 4°C for 12 h. After washing, the primary antibodies were incubated with Goat Anti-Rabbit IgG H&L (HRP) (ab205718, 1:30000, Abcam) for 2 h at 37°C. Subsequently, the protein bands were visualized with enhanced chemiluminescence (ECL) substrates (Beyotime).

Cell culture and treatments

Human normal lung epithelial cells (BEAS-2B) were obtained from Kanglang Biotechnology Co., Ltd. (Shanghai, China). Human lung carcinoma cells (95D) were acquired from the Huaao Biomedical Technology Co., Ltd. (Nanjing, China). Human lung cancer cell lines (A549, H1650, and H1299) were acquired from Merck Millipore (Billerica, MA, USA). The 95D, H1650, and H1299 cells were cultivated in RPMI-1640 medium (Beyotime) and the BEAS-2B and A549 cells were cultured in DMEM medium (Beyotime). Besides, the medium contained 10% fetal bovine serum (FBS) (Beyotime) and 1% penicillin/streptomycin (Sigma, St. Louis, MO, USA).

Small interfering RNAs (siRNAs) targeting SETDB1 (si-SETDB1#1 and si-SETDB1#2) or USP7 (si-USP7), siRNA negative control (si-NC), and overexpression vector for SETDB1 or NRF2 (OE-SETDB1; OE-NRF2) were designed by GenePharma (Shanghai, China). The cells were transfected with siRNAs or overexpression vectors using Lipofectamine 3000 (Invitrogen) according to the manufacturer's instructions.

For functional assys, H1650 and H1299 cells were treated with si-NC, si-SETDB1#1, si-SETDB1#2, si-USP7, si-USP7+OE-SETDB1. To explore the type of cell death involved, cells were treated with si-NC, si-SETDB1#1, si-SETDB1#1+Z-VAD-FMK (apoptosis inhibitor; 5 μM), si-SETDB1#1+Necrostatin-1 (necroptosis inhibitor; 10 μM), or si-SETDB1#1+Ferrostatin-1 (ferroptosis inhibitor; 1 μM) to examine the cell viability.

To evaluate USP7 inhibition, H1650 and H1299 cells were treated with 20 μM P22077 (USP7 inhibitor; Selleck Chemicals, Houston, TX, USA) or dimethyl sulfoxide (DMSO) for 24 h, after which the cells were harvested to detect SETDB1 expression.

For proteasome inhibition experiments, H1650 and H1299 cells were transfected with si-USP7 and subsequently treated with 10 μM MG132 (a specific proteasome inhibitor; Selleck Chemicals) before harvesting for Western blot analysis of SETDB1 expression

Measurement of cell viability

The H1650 and H1299 cells were seeded into 96-well microplates and subsequently subjected to different treatments. After that, the 3-(4,5-dimethylthiazol-2-yl)-2,5-diphenyltetrazolium bromide (MTT) solution (Sigma) was added to 96-well plates and incubated at 37°C for 4 h in a 5% CO_2 incubator. After dissolving the formazan crystals in dimethyl sulfoxide (DMSO), the absorbance was measured at 570 nm using a microplate reader.

Detection of cell proliferation

Cells were seeded into 6-well microplates and treated as required. Subsequently, the cells were reacted with 5-ethynyl-2'-deoxyuridine (EdU) (Beyotime) working fluid for 2 h. After removing the medium, 4% paraformaldehyde (Beyotime) was added to fix the cells for 15 min. Then, cells were washed and treated with the permeabilization solution (Beyotime) for 15 min. Next, cells were reacted with click reaction liquid at 37°C for 30 min in a dark environment. Nuclei were counterstained with DAPI for 6 min, and the cell proliferation was assessed using a fluorescence microscope. The percentage of EdU-positive cells relative to DAPI-positive cells was calculated.

Detection of cell apoptosis

Cell apoptosis was examined using Annexin-FITC Apoptosis Detection Kit (Sigma). Briefly, the cells were inoculated into 6-well microplates and transfected with the indicated siRNA and overexpression vector. The harvested cells were resuspended in the binding buffer and incubated with 5 μl of Annexin V-FITC and 10 μl of propidium iodide (PI) for

15 min in the dark. Finally, a FACS Canto II flow cytometer (BD Biosciences, Franklin Lakes, NJ, USA) was employed to examine the number of apoptotic cells.

Detection of cell invasion

The 24-well Transwell plates (Corning, NY, USA) with Matrigel-coated chamber inserts (8.0-μm pore size) were used to examine the ability of cell invasion. The cells with different treatments were suspended in serum-free RPMI-1640 medium and seeded into the upper chamber. The medium containing 10% FBS was plated into the bottom chamber. After incubation for 24 h, the cells that had invaded through the membrane were fixed with 4% paraformaldehyde for 10 min. Subsequently, 0.1% crystal violet was used to stain the cells for 30 min. Finally, the number of invasive cells from 5 random fields was examined using the microscope.

Sphere formation assay

Transfected cells were plated in 96-well ultra-low plates and cultured in serum-free DMEM/F12 medium supplemented with 20 ng/ml EGF, 20 ng/mL bFGF, and 2% B27. After 14 days of culture under standard conditions (5% CO_2, 37°C), tumor spheres were counted under a microscope.

Ferrous iron detection

After treated with different treatments, the cells underwent homogenization in 5× volumes of iron assay buffer on ice and then were centrifuged for 10 min at 4°C to obtain the supernatant. Then, the ferrous iron level was analyzed using an iron assy kit (Abcam) following the manufacturer's guideline.

Measurement of malondialdehyde (MDA)

The MDA levels were measured using the MDA assay kit (Beyotime). The cells with different treatments were lysed using RIPA solution (Invitrogen). Subsequently, the cell lysate was centrifuged (12000×g, 10 min) and then the supernatant was obtained. The protein concentration was detected using a BCA assay kit (Beyotime). The supernatant was mixed with MDA working solution (Beyotime) and then heated for 15 min at 100°C. After cooling, the samples were centrifuged for 10 min, and the 200 μl of the supernatant was added to a 96-well microplate. The absorbance was measured at 532 nm using a microplate reader.

Measurement of glutathione (GSH)

In short, the treated cells were reacted with lysis buffer and the lysates were centrifuged (12000×*g*, 10 min) to harvest the supernatant. The GSH levels were examined using a GSH assay kit (Beyotime) following the instructions of GSH kits.

Measurement of reactive oxygen species (ROS)

Intracellular ROS production was examined using a ROS assy kit (Beyotime). After different treatments, the medium was discarded, and cells were reacted with the 10 μmol/l DCFH-DA in serum-free medium for 1 h at 37°C in a humidified incubator with 5% CO_2. Following that, the cells were washed using medium without FBS. Finally, the ROS levels were assessed using the fluorescence microscope.

Co-immunoprecipitation (Co-IP) assay

Cells were lysed using IP lysis buffer (Beyotime) and centrifugated to harvest the supernatant. A small portion of the supernatant was used as the Input control. The remaining supernatant was incubated with anti-USP7 (ab264422, Abcam), anti-SETDB1 (ab300573, Abcam), or normal IgG (ab109489, Abcam) for 12 h at 4°C, followed by incubation with ProteinA/G magnetic beads (Thermo Fisher Scientific) at 4°C for 2 h. Magnetic beads were collected by magnetic stand and the supernatant was discarded. After washing, the beads were resuspended in SDS loading buffer and boiled at 100°C for 5 min. The eluted immunocomplexes was collected for Western blot analysis.

GST pull down assay

The GST pull down kit (Absin, Shanghai, China) was used to perform GST pull down assay. First, GST and GST-USP7 fusion proteins were expressed in *E. coli* and purified. Recombinant SETDB1 protein was expressed and purified separately. For pull-down assay, GST (control group) or GST-USP7 (experimental group) was mixed with Glutathione MagBeads and incubated for 2 h at 4°C. After washing, the purified SETDB1 protein was then added and incubated overnight at 4°C to promote protein-protein interaction. The beads were washed five times, and the bound complexes were eluted by boiling in SDS loading buffer for 10 min and analyzed by Western blot.

Protein stability assay

After transfected with si-USP7 or si-NC, the cells were cultured in medium containing 20 μg/ml cycloheximide (CHX; Selleck Chemicals) for 0, 2, 4, 6, or 8 h. The cells were collected to detect the SETDB1 protein levels using Western blot.

Ubiquitination detection

Transfected (si-NC or si-USP7) cells were lysed to obtain the cell lysates. A small portion of each lysates was used as

the Input for detecting SETDB1. The remaining lysates were incubated with anti-SETDB1 (ab300573, Abcam) at 4°C for 12 h, and then combined with prewashed A/G magnetic beads for 4 h at 4°C. The magnetic beads were washed and eluted with 2×SDS buffer. Finally, the proteins were examined using Western blot assay with anti-SETDB1 (ab300573, Abcam) or anti-Ub (ab134953).

To determine the type of ubiquitin chain conjugated to SETDB1 by USP7, H1650 cells were co-transfected with SETDB1 together with HA-tagged wild-type ubiquitin (WT), K48-only ubiquitin (K48), or K63-only ubiquitin (K63), with or without si-USP7 co-transfection. SETDB1 ubiquitination was then analyzed by IP-Western blot as described above.

Tumor xenograft models

BALB/c nude mice (aged 7 weeks) were acquired from SiPei-Fu Biotechnology Co., Ltd. (Beijing, China). Subsequently, the mice were assigned to 3 groups: sh-NC ($n = 5$), sh-USP7 ($n = 5$), and sh-USP7+OE-SETDB1 ($n = 5$). H1299 cells stably transfected with sh-NC, sh-USP7, or sh-USP7+OE-SETDB1 were resuspended in PBS at a density of 1×10^7 cells/ml and injected subcutaneously into the right flank of each mouse). From day 8 post-injection, tumor volumes were detected every 5 days and calculated using the formula: $V = (\text{length} \times \text{width}^2)/2$. On day 28, mice were sacrificed, and xenografts were removed, weighed and collected for immunohistochemistry (IHC) or Western blot assays. The animal experimental procedures were permitted by Animal Care and Use Committee of Tangdu Hospital of Air Force Military Medical University.

To determine whether the tumor-suppressive effect of USP7 knockdown is mediated by ferroptosis, mice divided into sh-NC, sh-USP7, or sh-USP7+Fer-1 ($n = 5$ *per* group). For the Fer-1 treatment group, Fer-1 (10 mg/kg) was administered via intraperitoneal injection daily starting from day 8 post-injection. The sh-NC and sh-USP7 groups received an equal volume of DMSO.

IHC assay

Mouse tumor tissues were fixed in paraformaldehyde, embedded in paraffin, and sectioned to slices with 4 μm thickness. After deparaffinization, rehydration, antigen retrieval, and blocking, sections were incubated with anti-proliferating cell nuclear antigen (PCNA) (ab92552, Abcam), anti-matrix metallopeptidase 2 (MMP2) (ab308346, Abcam), or anti-SETDB1 (ab228575, Abcam) for 12 h at 4°C, and then the secondary horseradish peroxidase (HRP)-conjugated anti-rabbit IgG (ab205718, Abcam) was added to incubate for 1 h. After staining with diaminobenzidine and hematoxylin, the sections were examined by microscopy.

Statistical analysis

All experiments were performed at least 3 times and statistical analyses were analyzed using GraphPad Prism 9.50 software (GraphPad Software, Boston, MA, USA). Data were shown as the mean ± standard deviation. Differences were compared by Student's *t*-test for two groups or analysis of variance (ANOVA) followed by Tukey's test for multiple groups. Kaplan-Meier curves and log-rank test were used to evaluate the overall survival in NSCLC patients. A p value less than 0.05 was regarded as statistically significant.

Results

Expression of SETDB1 is elevated in NSCLC tissues and cells

To explore the role of SETDB1 in NSCLC, its expression in NSCLC patients was analyzed. Based on TCGA, CPTAC, and ENCORI databases, SETDB1 expression was highly expressed in LUAD tissues (Fig. 1A–C). TNMplot database showed that SETDB1 expression was increased in lung cancer tissues compared with adjacent normal tissues (Fig. 1D). qRT-PCR results showed that SETDB1 mRNA was highly expressed in our collected NSCLC tissues compared with corresponding normal tissues (Fig. 1E). Additionally, NSCLC patients with higher expression of SETDB1 showed a lower overall survival (Fig. 1F). Western blot results demonstrated that SETDB1 protein expression was up-regulated in NSCLC tissues when compared with the corresponding normal tissues (Fig. 1G). In 95D, A549, H1650, and H1299 cells, SETDB1 expression was increased compared with the BEAS-2B cells (Fig. 1H). In summary, SETDB1 expression was increased in NSCLC tissues and cell lines.

Silencing SETDB1 hinders NSCLC cell viability, proliferation, invasion, and sphere formation ability, and promotes apoptosis

After H1299 and H1650 cells were transfected with si-SETDB1#1 or si-SETDB1#2, SETDB1 protein levels were significantly decreased (Fig. 2A). Silencing SETDB1 inhibited viability of H1299 and H1650 cells (Fig. 2C), and this effect was significantly weakened by Z-VAD-FMK/Ferrostatin-1 rather than Necrostatin-1 (Fig. S1), suggesting the involvement of apoptosis and ferroptosis. Silencing SETDB1 suppressed the proliferation of H1299 and H1650 cells (Fig. 2C). The apoptosis was promoted in SETDB1-silenced H1299 and H1650 cells when compared with the si-NC group (Fig. 2D). Additionally, cell invasion ability was suppressed by silencing SETDB1 (Fig. 2E). Knockdown of SETDB1 suppressed the

sphere formation efficiency of H1299 and H1650 cell (Fig. 2F). Taken together, SETDB1 promotes NSCLC cell viability, proliferation, invasion, and sphere formation ability, and inhibits cell apoptosis.

SETDB1 knockdown induces ferroptosis in NSCLC cells

A previous study has reported that SETDB1 is related to ferroptosis (Fan et al. 2025). Therefore, the effects of SETDB1 knockdown on ferroptosis in NSCLC were examined. As shown in Fig. 3A and B, Fe^{2+} and MDA levels in H1650 and H1299 cells were promoted by si-SETDB1#1 and si-SETDB1#2. Silencing SETDB1 led to a significant reduction of GSH production in NSCLC cells (Fig. 3C). Down-regulation of SETDB1 contributed to the increase of ROS levels (Fig. 3D). Additionally, down-regulation of SETDB1 decreased GPX4 expression levels (Fig. 3E). In summary, suppressing SETDB1 promotes ferroptosis in NSCLC cells.

USP7 enhances the stability of SETDB1 protein

Through analyzing UbiBrowser database, SETDB1 was predicted to be a potential substrate of USP7 (Fig. 4A). As shown in Fig. S2A and B, the USP7 expression was positively correlated with SETDB1 expression in ENCORI and GEPIA databases. In our collected patients, USP7 mRNA expression was increased in NSCLC tissues relative to normal tissues (Fig. S2C). Also, USP7 mRNA expression in our NSCLC tissues was positively correlated with the expression of SETDB1 mRNA (Fig. S2D). Subsequently, H1650 and H1299 cells were treated with P22077 (USP7 inhibitor), and the results demonstrated that SETDB1 protein levels were decreased when compared with the DMSO group (Fig. 4B). USP7 protein levels in H1650 and H1299 cells were decreased by si-USP7 (Fig. 4C). Compared with the si-NC group, silencing USP7 decreased SETDB1 protein expression in H1650 and H1299 cells, while MG132 (a specific inhibitor of proteasome) reversed this effect

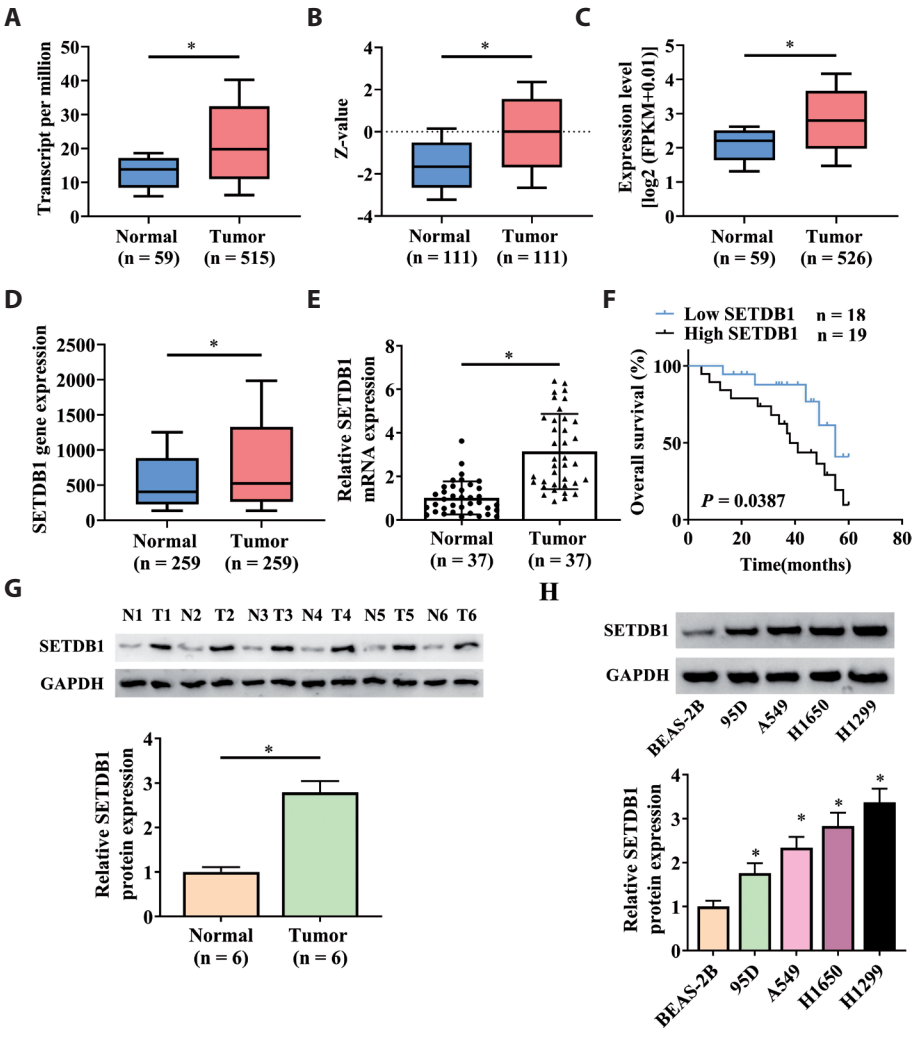

Figure 1. Expression of SETDB1 is elevated in NSCLC tissues and cells. The expression of SETDB1 in lung tissues was analyzed using TCGA (**A**), CPTAC (**B**), ENCORI (**C**), and TNMplot (**D**) databases. **E.** qRT-PCR was used to detect the SETDB1 mRNA levels in NSCLC tissues (n = 37) and normal tissues (n = 37). * p < 0.05 by paired t test. **F.** Kaplan-Meier survival analysis was used to analyze the relationship between SETDB1 expression and overall survival of NSCLC patients. p = 0.0387 by Log-rank test. **G.** The protein levels of SETDB1 were examined in NSCLC tissues (n = 6) and normal tissues (n = 6) using Western blot. * p < 0.05 by paired t test. **H.** SETDB1 mRNA expression in BEAS-2B, 95D, A549, H1650, and H1299 cells was detected using Western blot. * p < 0.05 by one-way ANOVA.

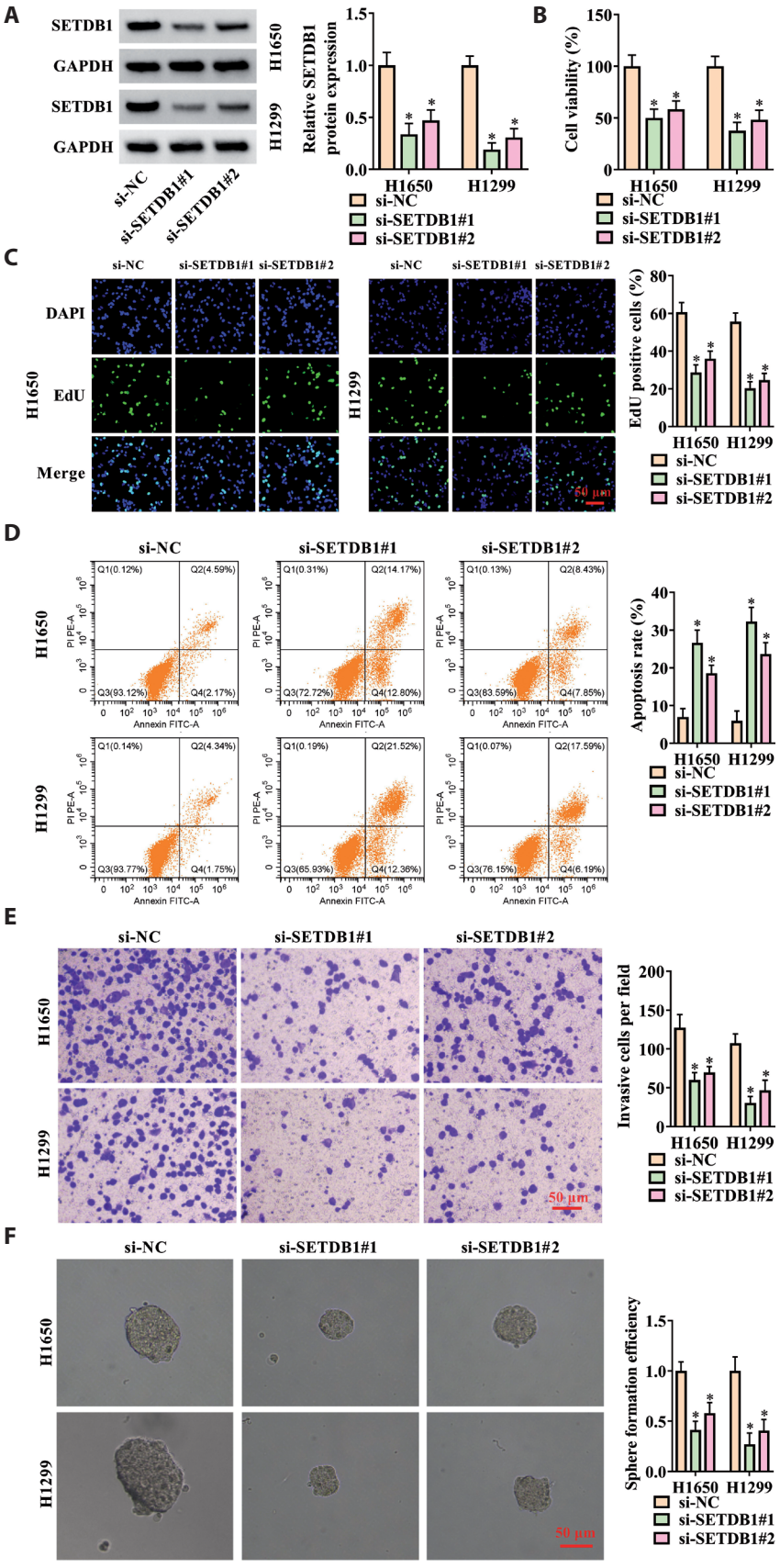

Figure 2. Silencing SETDB1 inhibits NSCLC cell viability, proliferation, invasion, and sphere formation efficiency, and promotes apoptosis. H1650 and H1299 cells were transfected with si-NC, si-SETDB1#1, or si-SETDB1#2. **A.** The SETDB1 protein levels were examined using Western blot. **B.** The cell viability was analyzed using MTT assay. **C.** Cell proliferation was detected by EdU assay. The apoptosis (**D**) and invasion (**E**) were analyzed using flow cytometry and transwell assays, respectively. **F.** The sphere formation efficiency was tested using sphere formation assay. * $p < 0.05$ by one-way ANOVA.

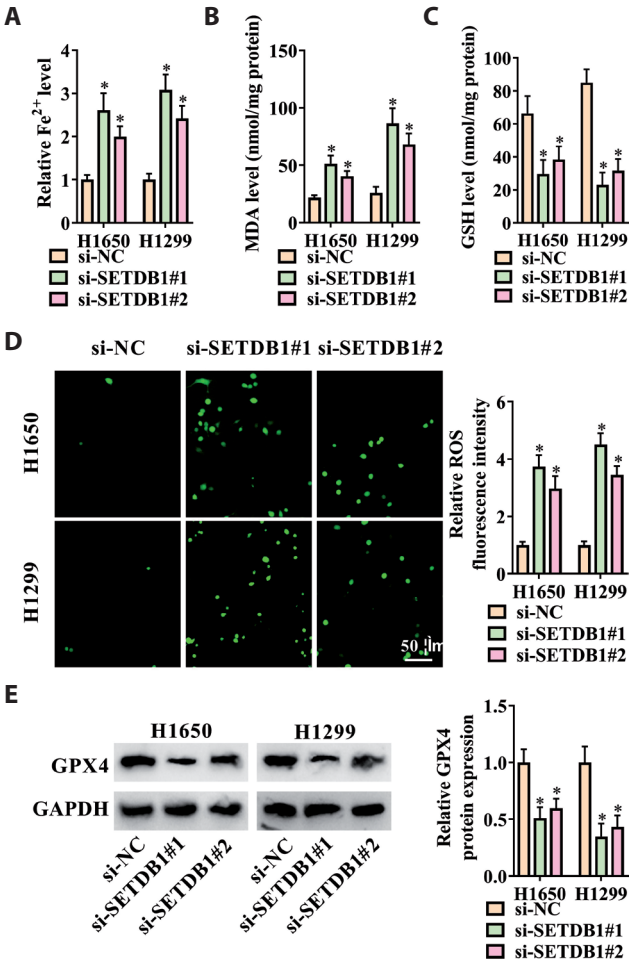

Figure 3. SETDB1 knockdown induces ferroptosis in NSCLC cells. After H1650 and H1299 cells were transfected with si-NC, si-SETDB1#1, or si-SETDB1#2, the Fe^{2+} (**A**), MDA (**B**), GSH (**C**), and ROS (**D**) levels were examined using corresponding assay kits. **E.** The protein expression of GPX4 was determined using Western blot. * $p < 0.05$ by one-way ANOVA.

(Fig. 4D). In addition, Co-IP assay showed the endogenous interaction between USP7 and SETDB1 in NSCLC cells (Fig. 4E). GST pull down results showed that USP7 could directly interact with SETDB1 protein (Fig. S3). To further evaluate whether USP7 affects SETDB1 stability, si-NC- or si-USP7-transfected cells were treated with CHX. The results indicated that silencing USP7 decreased the half-life of SETDB1 (Fig. 4F). Moreover, Western blot result demonstrated that the ubiquitination level of SETDB1 protein was increased by USP7 silencing (Fig. 4G). USP7 knockdown markedly enhanced K48-linked ubiquitination of SETDB1, but did not affect its K63-linked ubiquitination (Fig. S4), indicating that USP7 specifically targets K48-linked polyubiquitin chains on SETDB1. Overall, USP7 promotes the stability of SETDB1 by decreasing its ubiquitination in NSCLC cells.

USP7 knockdown hinders NSCLC cell biological behaviors via silencing SETDB1

As shown in Figure 5A, SETDB1 protein levels were increased in NSCLC cells with OE-SETDB1. Compared with the OE-NC group, the cell viability and proliferation of H1650 and H1299 cells were reduced in the si-USP7 group, which was increased again by OE-SETDB1 co-transfection (Fig. 5B,C). OE-SETDB1 reversed si-USP7-induced apoptosis in H1650 and H1299 cells (Fig. 5D). As shown in Fig. 5E, USP7 knockdown repressed H1650 and H1299 cell invasion, while OE-SETDB1 co-transfection weakened this action. The sphere formation ability in the si-USP7 group was repressed compared with the si-NC group, but SETDB1 overexpression reversed this effect (Fig. 5F). Overexpression of SETDB1 abolished si-USP7-induced promotion of Fe^{2+} and MDA levels (Fig. 5G,H). The GSH levels in si-USP7 group were suppressed, while OE-SETDB1 remitted this action (Fig. 5I). Silencing USP7 facilitated ROS production in NSCLC cells, but this action was abated by OE-SETDB1 (Fig. 5J). To sum up, USP7 knockdown inhibits NSCLC cell viability, proliferation, invasion, and sphere formation efficiency and facilitates apoptosis *via* silencing SETDB1.

USP7 knockdown inhibits NRF2, SLC7A11, and GPX4 levels by silencing SETDB1

Ferroptosis is a type of programmed cell death that is characterized by lipid peroxidation (Xue et al. 2023). Impaired GSH metabolism underlies ferroptosis, including GSH deficiency due to SLC7A11 dysfunction, which in turn compromises GPX4 activity and leads to direct GPX4 inhibition (Koppula et al. 2021). Besides, SLC7A11 and GPX4 are transcriptionally regulated by NRF2 (Abdelgawwad El-Sehrawy et al. 2025). Thus, we explored whether USP7/STEDB1 regulates ferroptosis through the NRF2/SLC7A11/GPX4 axis. As shown in Fig. 6A, si-USP7 inhibited NRF2 expression in H1650 and H1299 cells, while overexpression of SETDB1 abolished this action. Besides, OE-SETDB1 remitted si-USP7-induced inhibition effect on SLC7A11 and GPX4 levels (Fig. 6B,C). NRF2 was successfully overexpressed in H1650 and H1299 cells by transfection with OE-NRF2 (Fig. S5A). Importantly, si-SETDB1-mediated inhibition of cell ability and invasion was rescued by NRF2 overexpression (Fig. S5B,C). Additionally, si-SETDB1-mediated ROS release was alleviated by OE-NRF2 (Fig. S5D). Overall, USP7 silencing induces ferroptosis in NSCLC cells by suppressing the NRF2/SLC7A11/GPX4 axis via regulation of SETDB1.

In vivo, USP7 promotes NSCLC tumor growth through regulating SETDB1

Next, we analyzed the association of USP7 and SETDB1 in regulating the malignant growth of NSCLC cells using xenograft tumor models. Compared with the sh-NC group, USP7 knockdown inhibited USP7 protein expression in tumors; however, overexpression of SETDB1 did not change USP7 expression in tumors when compared with the sh-USP7 group (Fig. S6A). Silencing USP7 suppressed the tumor growth, which was weakened by OE-SETDB1/Ferrostatin-1 (Fig. 7A,B and Fig. S6B,C). Additionally, compared with the sh-NC group, silencing USP7 hindered SETDB1 expression in xenografts, but overexpression of SETDB1 reversed this action (Fig. 7C). Notably, SETDB1 overexpression abrogated sh-USP7-induced repression of ferroptosis-related proteins (NRF2, SLC7A11, and GPX4) (Fig. 7D). IHC results also demonstrated that silencing USP7 reduced PCNA, MMP2, and SETDB1 levels, which were increased by SETDB1 overexpression (Fig. 7E). Altogether, knockdown of USP7 hinders *in vivo* tumor growth of NSCLC by suppressing SETDB1.

Discussion

Globally, NSCLC remains the leading cause of cancer-related deaths, with high recurrence rates (Oikawa et al. 2024). Although certain progress has been made in its treatment, challenges such as distant metastasis, drug resistance, and local recurrence persist, resulting in poor outcomes for some patients (Alduais et al. 2023; Yang Y et al. 2024). Therefore, the underlying mechanism driving NSCLC development needs to be further explored.

SETDB1 is a crucial H3K9 methyltransferase that participates in multiple regulatory processes, including cell proliferation, migration, apoptosis, progression, and survival (Prashanth et al. 2024). SETDB1 levels were increased in a variety of human cancers, contributing to tumor growth and metastasis (Hassanie and Penteado 2024). For example,

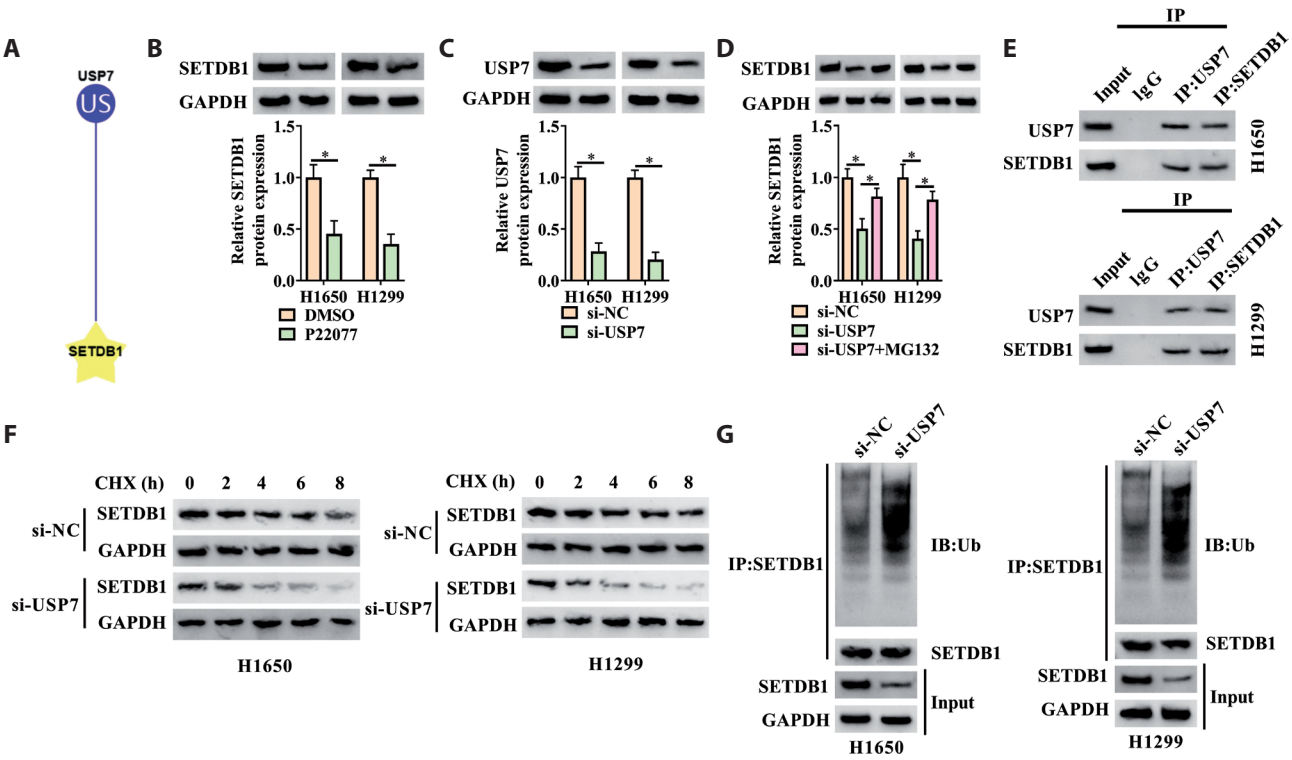

Figure 4. USP7 enhances the stability of SETDB1 protein. **A.** Ubibrowser database predicts USP7 as a potential deubiquitinase of SETDB1. **B.** After H1650 and H1299 cells were treated with DMSO or P22077, the SETDB1 protein levels were detected using Western blot. **C.** Western blot assay was employed to analyze USP7 protein levels in NSCLC cells with si-USP7 or si-NC transfection. **D.** The SETDB1 expression in si-NC, si-USP7, or si-USP7+MG132 groups was examined by Western blot. **E.** Co-IP assay was carried out to detect the interaction between USP7 and SETDB1 in NSCLC cells. **F.** The half-life of SETDB1 protein was evaluated by CHX assay after USP7 knockdown. **G.** After the cells were transfected with si-NC or si-USP7, the ubiquitination of SETDB1 was detected by IP and Western blot. * $p < 0.05$ by unpaired t test or one-way ANOVA.

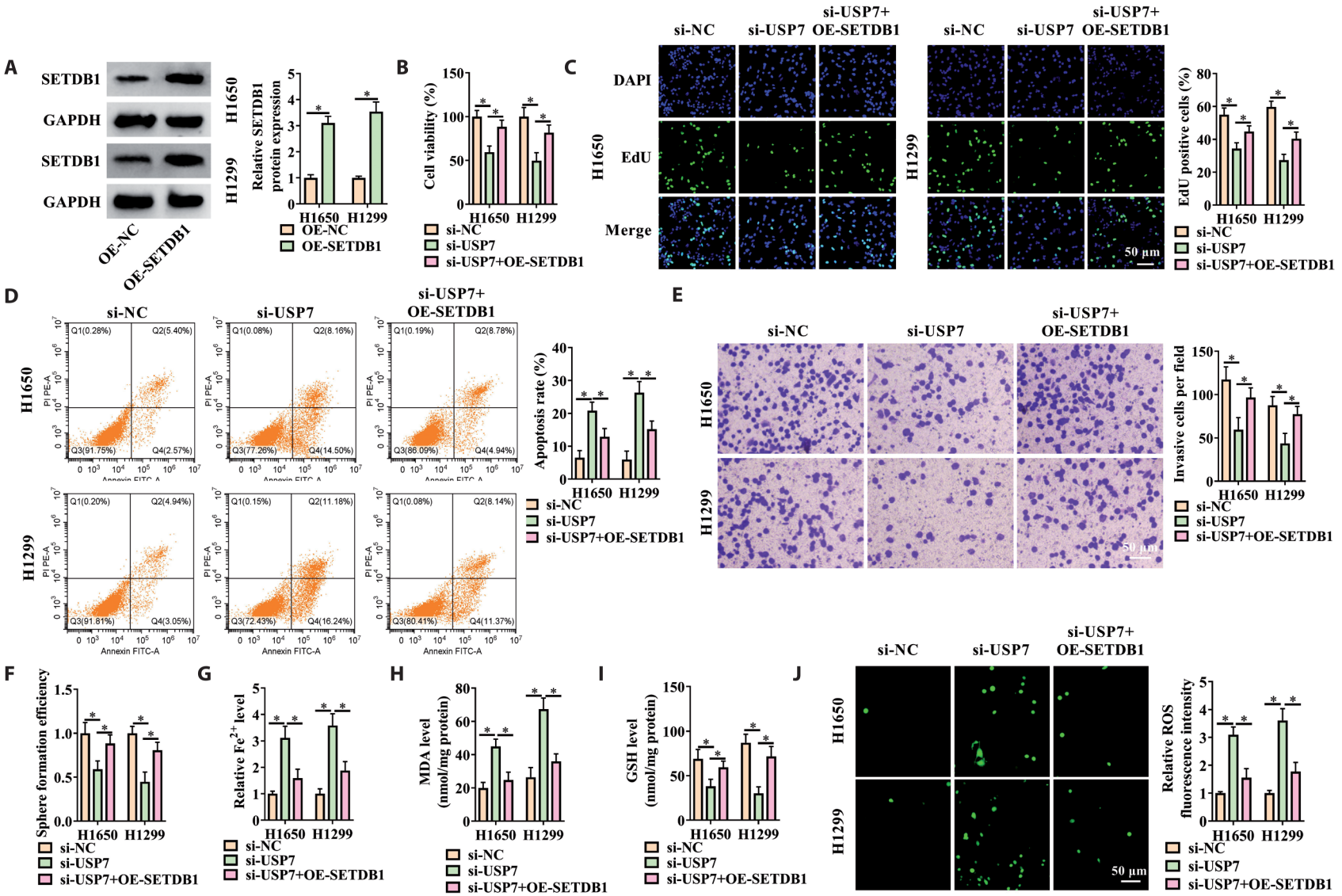

Figure 5. USP7 knockdown hinders NSCLC cell biological behaviors *via* silencing SETDB1. **A.** In H1299 and H1650 cells with OE-NC and OE-SETDB1 transfection, the SETDB-1protein expression was detected by Western blot. (B-J): H1299 and H1650 cells were transfected with si-NC, si-USP7, or si-USP7+OE-SETDB1. **B.** Cell viability was analyzed using MTT assay. **C.** The cell proliferation was examined using EdU assay. **D.** Flow cytometry assay was used to analyze the cell apoptosis. **E.** The invasion ability of cells was analyzed using transwell assay. **F.** The sphere formation efficiency in each group was tested using sphere formation assay. The Fe^{2+} (**G**), MDA (**H**), GSH (**I**), and ROS (**J**) levels were examined using corresponding assay kits. * $p < 0.05$ by by unpaired *t* test or one-way ANOVA.

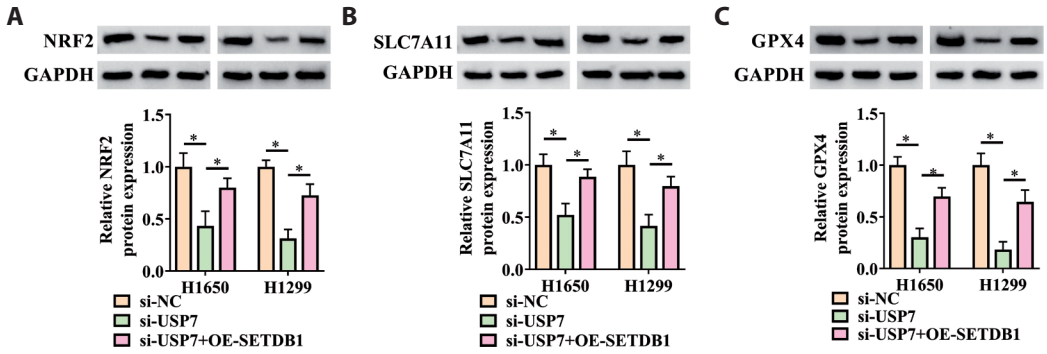

Figure 6. USP7 knockdown inhibits NRF2, SLC7A11, and GPX4 protein levels by silencing SETDB1. After NSCLC cells were transfected with si-NC, si-USP7, or si-USP7+OE-SETDB1, the expression of NRF2 (**A**), SLC7A11 (**B**), and GPX4 (**C**) was analyzed by Western blot. * $p < 0.05$ by one-way ANOVA.

SETDB1 was up-regulated in colorectal cancer, and its silencing hindered invasion and metastasis (Li et al. 2023). In our study, SETDB1 was promoted in NSCLC tissues and cells, suggesting its association with disease progression. Additionally, SETDB1 overexpression in NSCLC cells facilitated *in vitro* proliferation and xenograft tumor growth through different pathways (Strepkos and Markouli 2021), and enhanced the migration and invasion abilities *via* strengthening the formation of invasive pseudopodia (Ueshima and Fang 2022). Elevated level of SETDB1 also increased clonogenic growth, correlating with NSCLC tumor expansion (Sun et al. 2015). Notably, gene amplification of SETDB1 has been implicated in the onset of human lung tumorigenesis (Rodriguez-Paredes et al. 2014). Consistently, our findings demonstrated that SETDB1 knockdown suppressed malignant behaviors of NSCLC, corroborating these previous reports.

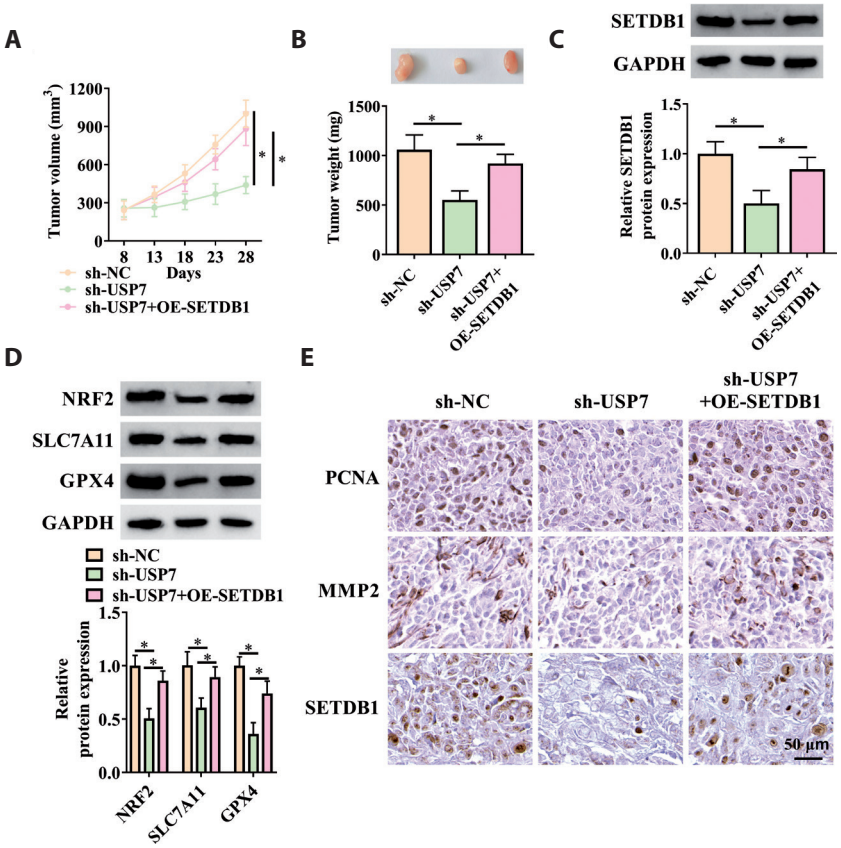

Figure 7. *In vivo*, USP7 promotes NSCLC tumor growth through regulating SETDB1. The mice were divided into three groups according to different treatments (sh-NC group, sh-USP7 group, and sh-USP7+OE-SETDB1 group). **A.** The tumor volume was analyzed. * $p < 0.05$ by two-way ANOVA. **B.** The tumor weight was analyzed. * $p < 0.05$ by one-way ANOVA. **C.** SETDB1 protein expression was examined using Western blot. * $p < 0.05$ by one-way ANOVA. **D.** The NRF2, SLC7A11, and GPX4 protein levels were examined using Western blot. * $p < 0.05$ by one-way ANOVA. **E.** IHC assay was performed to test the PCNA, MMP2, and SETDB1 expression.

Lipid peroxidation is a characteristic of ferroptosis, a form of programmed cell death (Park et al. 2021). Ferroptosis is related to tumorigenesis and progression (Mou et al. 2019; Stockwell 2022). Interestingly, Liu *et al.* demonstrated that silencing SETDB1 enhanced TGF-β-induced ferroptosis (Liu et al. 2022b), raising the possibility that SETDB1 may regulate ferroptosis to influence NSCLC progression. In line with this hypothesis, our findings demonstrated that SETDB1 knockdown promoted ferroptosis in NSCLC cells, consistent previous observations (Fan et al. 2025).

Ubiquitination is a protein modification with complicated mechanism, controlled by E3 ubiquitin ligases and deubiquitinating enzymes, and is extensively implicated in a number of physiological and pathological processes (Rape 2018; Liu et al. 2022a). Deubiquitination-mediated inhibition of proteolysis plays a crucial role in human tumorigenesis (Sun et al. 2020; Zou et al. 2025). USP7 is a well-known deubiquitinating enzyme. He et al. showed that USP7 overexpression promoted NSCLC cell growth and metastasis. as well as xenograft growth in nude mice (He et al. 2023). Although the oncogenic potential of USP7 in NSCLC has been extensively documented, our understanding of its target substrates remains limited. Through bioinformatics analysis and experimental validation, we demonstrated that USP7 enhanced the protein stability of SETDB1 through deubiquitination. Additionally, USP7 facilitated proliferation of NSCLC cells by promoting KRAS stability through ubiquitination (Huang et al. 2024). USP7 overexpression contributed to NSCLC cell proliferation, migration, and tumor growth *in vivo* (He et al. 2023), which was consistent with our results that si-USP7 repressed NSCLC progression. Moreover, overexpression of SETDB1 abolished si-USP7-induced effect on NSCLC malignant phenotypes and ferroptosis, implying the USP7/SETDB1 regulatory axis in NSCLC. At the same time, USP7 knockdown hindered NSCLC tumor growth *in vivo* through regulating SETDB1. Furthermore, Rodriguez-Paredes reported that high expression of SETDB1 in NSCLC was associated with gene locus amplication (Rodriguez-Paredes et al. 2014). This represents another layer of critical regulation underlying elevated SETDB1 protein levels in NSCLC, suggesting that multiple mechanisms-including gene amplification and protein stability control-may collectively contribute to SETDB1 dysregulation in cancer. This aspect warrants further investigation in future studies.

The precise regulatory link between SETDB1 and the core ferroptosis pathway warrants further discussion. In our study, SETDB1 overexpression overturned si-USP7-mediated inhibition on NRF2, SLC7A11, and GPX4 protein expression. This aligns with a previous report that overexpression of SETDB1 in lung adenocarcinom promotes the expression of GPX4 (Fan et al. 2025). However, the exact molecular mechanism, particularly whether SETDB1 directly regulates ferroptosis-related genes at the chromatin level, remains a key unresolved question. As a histone methyltransferase primarily catalyzing H3K9 trimethylation (H3K9me3), it is plausible that SETDB1 modulates the NRF2/SLC7A11/GPX4 pathway through chromatin-based mechanisms. One possibility is direct transcriptional regulation, whereby SETDB1 binds to promoter regions of these genes. Its role may be context-dependent: while it might repress SLC7A11 transcription by depositing the repressive H3K9me3 mark at its promoter, as suggested by a study where SETDB1 inhibition enhanced SLC7A11 expression (Xiong et al. 2025), it could simultaneously or alternatively act as a co-activator for GPX4 transcription, potentially through interactions with other transcription factors or by maintaining a permissive chromatin state at its locus. Another possibility involves indirect regulation, where SETDB1 silences genes encoding negative regulators of the NRF2 pathway (eg. specific KEAP1 isoforms or microRNAs), thereby indirectly potentiating NRF2 activity and its downstream targets. The seemingly contradictory roles of SETDB1-inhibiting SLC7A11 transcription in one context while promoting GPX4 and overall pathway activity in another-highlight the context-dependent nature of epigenetic regulation in ferroptosis. The net effect of SETDB1 on ferroptosis sensitivity is likely determined by the integration of its influences on multiple downstream targets, including but not limited to the NRF2/SLC7A11/GPX4 axis. Future studies employing chromatin immunoprecipitation sequencing (ChIP-seq) for SETDB1 and H3K9me3, combined with transcriptomic analysis upon SETDB1 modulation, are essential to map its direct genomic targets and precisely define its mechanistic role in regulating ferroptosis defense.

This study has several limitations that point to future directions. First, the precise molecular mechanism by which SETDB1 regulates the NRF2/SLC7A11/GPX4 axis, whether direct or indirect, remains unclear. Second, while this study focused on ferroptosis, the involvement of other cell death pathways (eg. autophagy) and the therapeutic potential of pharmacological USP7 inhibition require futher investigation. Third, the *in vivo* validation in this study relied on subcutaneous xenograft models in immunodeficient mice. While this model provided initial proof-of-concept, it does not fully recapitulate the lung-specific tumor microenvironment or the critical immune interactions that may influence NSCLC progression and ferroptosis regulation. Future studies employing orthotopic lung tumor models, patient-derived xenografts, or immunocompetent systems will be essential to strengthen the physiological and translational relevance of the USP7-SETDB1-ferroptosis axis. Finally, the upstream signaling pathways, such as the promising mTOR pathway (Fan et al. 2022; Zhao and Fan 2024) and the role of the USP7-SETDB1 axis in the tumor immune microenvironment are unknown, which are crucial for translational relevance.

While this study delineates a linear USP7-SETDB1 regulatory axis, cancer progression is governed by complex and interconnected gene networks. Emerging large-scale functional genomics approaches offer powerful tools to transition from discrete pathway analysis to systematic interrogation of causal regulatory principles. For instance, integrating patient-derived models with scalable single-cell RNA profiling of pooled genetic screens (eg. Perturb-Seq) could comprehensively map the downstream transcriptional networks and synthetic lethal interactions orchestrated by USP7 and SETDB1 (Dixit et al. 2016; Xu et al. 2024). Applying such methodologies to NSCLC models would enable the unbiased discovery of key co-regulators and therapeutic vulnerabilities within the USP7-SETDB1-ferroptosis axis, accelerating the translation of these findings into novel combination therapies. In summary, USP7 inhibits ferroptosis and promotes NSCLC biological behaviors by stabilizing SETDB1 *via* deubiquitination. Our results suggest that SETDB1 and USP7 may serve as potential therapeutic target for NSCLC.

Data availability statement. Data is available from the corresponding author upon reasonable request.

Conflicts of interest. The authors declare that they have no conflicts of interest.

References

Abdelgawwad El-Sehrawy AAM, Al-dulaimi AA, Alkhathami AG, S RJ, Panigrahi R, Pargaien A, Singh U, Husseini A, Alnajar MJ (2025): NRF2 as a ferroptosis gatekeeper in colorectal cancer: implications for therapy. Naunyn Schmiedebergs Arch Pharmacol **398,** 16479-16506 https://doi.org/10.1007/s00210-025-04324-3

Al-Eidan A, Wang Y, Skipp P, Ewing RM (2022): The USP7 protein interaction network and its roles in tumorigenesis. Genes Dis **9,** 41-50 https://doi.org/10.1016/j.gendis.2020.10.004

Alduais Y, Zhang H, Fan F, Chen J (2023): Non-small cell lung cancer (NSCLC): A review of risk factors, diagnosis, and treatment. Medicine (Baltimore) **102,** e32899 https://doi.org/10.1097/MD.0000000000032899

Carreira LD, Oliveira RI (2023): Ubiquitin-specific protease 7 (USP7): an emerging drug target for cancer treatment. Expert Opin Ther Targets **27,** 1043-1058 https://doi.org/10.1080/14728222.2023.2266571

Dixit A, Parnas O, Li B, Chen J, Fulco CP, Jerby-Arnon L, Marjanovic ND, Dionne D, Burks T, Raychowdhury R, et al. (2016): Perturb-Seq: Dissecting molecular circuits with scalable single-cell RNA profiling of pooled genetic screens. Cell **167,** 1853-1866.e17 https://doi.org/10.1016/j.cell.2016.11.038

Fan J, Yuan Z, Burley SK, Libutti SK, Zheng XFS (2022): Amino acids control blood glucose levels through mTOR signaling. Eur J Cell Biol **101,** 151240 https://doi.org/10.1016/j.ejcb.2022.151240

Fan X, Zhu Q, Du C, Chen J, Su Y (2025): SNX30 inhibits lung adenocarcinoma cell proliferation and induces cell ferroptosis through regulating SETDB1. J Cardiothorac Surg **20,** 51 https://doi.org/10.1186/s13019-024-03298-2

Ferlay J, Colombet M, Soerjomataram I, Parkin DM, Piñeros M, Znaor A, Bray F (2021): Cancer statistics for the year 2020: An overview. Int J Cancer **149,** 778-789 https://doi.org/10.1002/ijc.33588

Hassanie H, Penteado AB (2024): SETDB1 as a cancer target: challenges and perspectives in drug design. RSC Med Chem **15,** 1424-1451 https://doi.org/10.1039/D3MD00366C

He Y, Jiang S, Zhong Y, Wang X, Cui Y, Liang J, Sun Y, Zhu Z, Huang Z, Mao X (2023): USP7 promotes non-small-cell lung cancer cell glycolysis and survival by stabilizing and activating c-Abl. Clin Transl Med **13,** e1509 https://doi.org/10.1002/ctm2.1509

Huang B, Cao D, Yuan X, Xiong Y, Chen B, Wang Y, Niu X, Tian R, Huang H (2024): USP7 deubiquitinates KRAS and promotes non-small cell lung cancer. Cell Rep **43,** 114917 https://doi.org/10.1016/j.celrep.2024.114917

Kandemir O, Demir F (2024): An investigation of the relationship between (18)F-FDG PET/CT parameters of primary tumors and lymph node metastasis in resectable non-small cell lung cancer. Curr Radiopharm **17,** 111-116 https://doi.org/10.2174/1874471016666230829100703

Koppula P, Zhuang L, Gan B (2021): Cystine transporter SLC7A11/xCT in cancer: ferroptosis, nutrient dependency, and cancer therapy. Protein Cell **12,** 599-620 https://doi.org/10.1007/s13238-020-00789-5

Lafuente-Sanchis A, Zúñiga Á, Galbis JM, Cremades A, Estors M, Martínez-Hernández NJ, Carretero J (2016): Prognostic value of ERCC1, RRM1, BRCA1 and SETDB1 in early stage of non-small cell lung cancer. Clin Transl Oncol **18,** 798-804 https://doi.org/10.1007/s12094-015-1440-6

Li W, Yang X, Liu X, Deng H, Li W, He X, Zhang W, Shen Y, Li X, Peng Q, et al. (2023): SETDB1 confers colorectal cancer metastasis by regulation of WNT/β-catenin signaling. Biochim Biophys Acta Gen Subj **1867,** 130377 https://doi.org/10.1016/j.bbagen.2023.130377

Liu J, Jin J, Liang T, Feng XH (2022a): To Ub or not to Ub: a regulatory question in TGF-β signaling. Trends Biochem Sci **47,** 1059-1072 https://doi.org/10.1016/j.tibs.2022.06.001

Liu T, Xu P, Ke S, Dong H, Zhan M, Hu Q, Li J (2022b): Histone methyltransferase SETDB1 inhibits TGF-β-induced epithelial-mesenchymal transition in pulmonary fibrosis by regulating SNAI1 expression and the ferroptosis signaling pathway. Arch Biochem Biophys **715,** 109087 https://doi.org/10.1016/j.abb.2021.109087

Mou Y, Wang J, Wu J, He D, Zhang C, Duan C, Li B (2019): Ferroptosis, a new form of cell death: opportunities and challenges in cancer. J Hematol Oncol **12,** 34 https://doi.org/10.1186/s13045-019-0720-y

Oikawa M, Hanada M, Nagura H, Takeuchi R, Miyazaki T, Doi R, Sato S, Matsumoto K, Kozu R (2024): Association between health-related quality of life and perioperative exercise capacity

in older postoperative patients with non-small cell lung cancer. J Thorac Dis **16,** 8300-8308
https://doi.org/10.21037/jtd-24-1265

Özdaş S (2019): Knockdown of SET domain, Bifurcated 1 suppresses head and neck cancer cell viability and wound-healing ability in vitro. Turk J Biol **43,** 281-292
https://doi.org/10.3906/biy-1903-71

Park MW, Cha HW, Kim J, Kim JH, Yang H, Yoon S, Boonpraman N, Yi SS, Yoo ID, Moon JS (2021): NOX4 promotes ferroptosis of astrocytes by oxidative stress-induced lipid peroxidation via the impairment of mitochondrial metabolism in Alzheimer's diseases. Redox Biol **41,** 101947
https://doi.org/10.1016/j.redox.2021.101947

Prashanth S, Radha Maniswami R, Rajajeyabalachandran G, Jegatheesan SK (2024): SETDB1, an H3K9-specific methyltransferase: An attractive epigenetic target to combat cancer. Drug Discov Today **29,** 103982
https://doi.org/10.1016/j.drudis.2024.103982

Rape M (2018): Ubiquitylation at the crossroads of development and disease. Nat Rev Mol Cell Biol **19,** 59-70
https://doi.org/10.1038/nrm.2017.83

Rodriguez-Paredes M, Martinez de Paz A, Simó-Riudalbas L, Sayols S, Moutinho C, Moran S, Villanueva A, Vázquez-Cedeira M, Lazo PA, Carneiro F, et al. (2014): Gene amplification of the histone methyltransferase SETDB1 contributes to human lung tumorigenesis. Oncogene **33,** 2807-13
https://doi.org/10.1038/onc.2013.239

Saha G, Ghosh MK (2025): The key vulnerabilities and therapeutic opportunities in the USP7-p53/MDM2 axis in cancer. Biochim Biophys Acta Mol Cell Res **1872,** 119908
https://doi.org/10.1016/j.bbamcr.2025.119908

Saha G, Roy S, Basu M, Ghosh MK (2023): USP7 – a crucial regulator of cancer hallmarks. Biochim Biophys Acta Rev Cancer **1878,** 188903
https://doi.org/10.1016/j.bbcan.2023.188903

Stockwell BR (2022): Ferroptosis turns 10: Emerging mechanisms, physiological functions, and therapeutic applications. Cell **185,** 2401-2421
https://doi.org/10.1016/j.cell.2022.06.003

Strepkos D, Markouli M (2021): Histone methyltransferase SETDB1: A common denominator of tumorigenesis with therapeutic potential. Cancer Res Treat **81,** 525-534
https://doi.org/10.1158/0008-5472.CAN-20-2906

Sun QY, Ding LW, Xiao JF, Chien W, Lim SL, Hattori N, Goodglick L, Chia D, Mah V, Alavi M, et al. (2015): SETDB1 accelerates tumourigenesis by regulating the WNT signalling pathway. J Pathol **235,** 559-70
https://doi.org/10.1002/path.4482

Sun T, Liu Z, Yang Q (2020): The role of ubiquitination and deubiquitination in cancer metabolism. Mol Cancer Res **19,** 146
https://doi.org/10.1186/s12943-020-01262-x

Ueshima S, Fang J (2022): Histone H3K9 methyltransferase SETDB1 augments invadopodia formation to promote tumor metastasis. Oncogene **41,** 3370-3380
https://doi.org/10.1038/s41388-022-02345-3

Wang C, Xia Z, Li Z, Ye F, Ji S, Lu C, Zhang H (2022): Expression of SET domain bifurcated histone lysine methyltransferase 1 and its clinical prognostic significance in hepatocellular carcinoma. J Clin Lab Anal **36,** e24090
https://doi.org/10.1002/jcla.24090

Wang Y, Su C, Liang X, Li X, Jing M, Wang Q, Huang R, Yin F, Zhang G, Liu T, et al. (2025): Diagnosis of PD-L1 related non-small cell lung cancer from micro-liters blood. Talanta **293,** 128077
https://doi.org/10.1016/j.talanta.2025.128077

Xiong C, Ling H, Huang Y, Dong H, Xie B, Hao Q, Zhou X (2025): AZD1775 synergizes with SLC7A11 inhibition to promote ferroptosis. Sci China Life Sci **68,** 204-218
https://doi.org/10.1007/s11427-023-2589-1

Xu Z, Sziraki A, Lee J, Zhou W, Cao J (2024): Dissecting key regulators of transcriptome kinetics through scalable single-cell RNA profiling of pooled CRISPR screens. Nat Biotechnol **42,** 1218-1223
https://doi.org/10.1038/s41587-023-01948-9

Xue Q, Yan D, Chen X, Li X, Kang R, Klionsky DJ (2023): Copper-dependent autophagic degradation of GPX4 drives ferroptosis. Autophagy **19,** 1982-1996
https://doi.org/10.1080/15548627.2023.2165323

Yang H, Sui L, Cai C, Chu H, Diao Y (2024): SETDB1 promotes progression through upregulation of SF3B4 expression and regulates the immunity in ovarian cancer. J Ovarian Res **17,** 34
https://doi.org/10.1186/s13048-024-01358-8

Yang W, Su Y, Hou C, Chen L, Zhou D, Ren K, Zhou Z, Zhang R, Liu X (2019): SETDB1 induces epithelial-mesenchymal transition in breast carcinoma by directly binding with Snail promoter. Oncol Rep **41,** 1284-1292
https://doi.org/10.3892/or.2018.6871

Yang Y, Wang J, Wang J, Zhao X, Zhang T, Yang Y, Pang J, Ou Q, Wu L, Xu X, et al. (2024): Unrevealing the therapeutic benefits of radiotherapy and consolidation immunotherapy using ctDNA-defined tumor clonality in unresectable locally advanced non-small cell lung cancer. Cancer Lett **582,** 216569
https://doi.org/10.1016/j.canlet.2023.216569

Zhao T, Fan J (2024): Nuclear mTOR signaling orchestrates transcriptional programs underlying cellular growth and metabolism. Cells **13,** 781
https://doi.org/10.3390/cells13090781

Zou Y, Guo Z, Rong R, Zhang H, Han S (2025): Exploration of atractylenolide III targeting MDM2/p53 axis in breast cancer cell progression based on network pharmacology, molecular docking and ubiquitination analysis. Current Proteomics **22,** 100016
https://doi.org/10.1016/j.curpro.2025.100016

Received: September 22, 2025
Final version accepted: February 24, 2026